Role of the image charge and electronic corrugation on charge-fraction azimuthal variations for keV Li and Na ions interacting with Cu(110) and Ag(110) under grazing incidence

M. Richard-Viard,* C. Bénazeth, P. Benoit-Cattin, P. Cafarelli, and N. Nieuwjaer
Laboratoire Collisions, Agrégats, Réactivité, UMR 5589, CNRS, Institut de Recherches sur les Systemes Atomiques et Moleculaires Complexes, Université Paul Sabatier Toulouse 3, 31062 Toulouse Cedex 9, France
(Received 19 January 2007; revised manuscript received 25 May 2007; published 31 July 2007)

The positive charge fraction resulting from charge exchange during the interaction of Li^+ and Na^+ ions on the Ag(110) and Cu(110) metal surfaces has been measured for different energies and incident azimuthal angles of the projectiles. Surprisingly, although metallic Cu and Ag are well described by the free-electron model, the positive charge fraction has been observed to vary significantly according to the azimuthal angle of incidence, for projectile energies lower than 4 keV and incidence angle below 5° with respect to the surface (grazing scattering conditions), and specifically around the low-index [001] and $[1\bar{1}0]$ directions. A detailed analysis of trajectory calculations for the Li/Cu(110) system allows one to distinguish between different types of trajectories (on tops, zigzags, and in rows), the relative importance of which varies rapidly with azimuthal angle. We obtain a good correlation between the observed azimuthal variation of the charge fraction and the mean value of the electronic density encountered by the projectile in the vicinity of the first atomic layers. We show that this short-range effect can be reflected on the observed variation of the charge fraction through the charge image effect on the trajectories. This effect is shown to be very sensitive to the electronic corrugation of the surface which is known to be low for Cu and Ag. Azimuthal experimental measurements thus appear to be a tool to characterize such low corrugations.

DOI: 10.1103/PhysRevB.76.045432 PACS number(s): 79.20.Rf, 79.60.Bm, 61.85.+p

I. INTRODUCTION

During the interaction of an ion with a metal surface, there is a coupling between the electronic states of the projectile and the continuum of metal states. This leads to the possibility of a charge exchange between the projectile and the surface, i.e., an electron jump between the projectile and the surface. Charge-transfer processes play an important role in gas-surface interactions; they are involved as an intermediate step in various reactions at surfaces and they directly determine the charge states of projectiles in scattered beams.[1,2] For projectiles with low electron-binding energies (negative ions and alkali atoms), the projectile-surface interaction is dominated by a resonant charge-transfer process,[3] which is characterized by one-electron transitions between the projectile states and metal valence-band states of the same energy.

Experimentally, the resonant charge-transfer process can be studied by the measurement of charge fractions after the interaction of projectiles with a surface (low-energy ion scattering). One way to analyze a possible influence of the surface corrugation on the charge-transfer process is to study the dependence of charge fractions with the azimuthal angle of incidence. Significant variations of charge fractions with the azimuthal angle of incidence have been observed during the scattering of projectiles off ionic insulators.[4,5] Since the charges are localized in an ionic crystal (strong electronic corrugation), links can be established between the azimuthal angle of incidence, the projectile trajectories, and the charge exchange process.[4] This process is helped by small projectile-target distances, the exchange being localized in the vicinity of ionic cores. Such links are less obvious when one considers scattering off metal surfaces, in particular, at grazing incidence. These surfaces have extended electronic states, and so the charge state of the projectile is mainly determined on its exit far from the surface so that any memory concerning charge transfer for small projectile-surface distances is lost.[6,7] Nevertheless, some experiments have shown that in quasi-binary-collision conditions, charge transfer with metal surfaces could depend on the trajectories of singly charged[8] or multicharged ionic[9] projectiles. In the case of low-energy grazing interactions, variations of the surviving ion's fraction with the crystallographic orientation have been reported in the case of Auger neutralization of He ions interacting with Ni(110).[10] In this paper, we present variations of the ion fraction with the crystallographic orientation in the case of alkali-ion neutralization by a resonant charge-transfer process with the Ag(110) and Cu(110) surfaces.

II. EXPERIMENT

A detailed description of the apparatus is given elsewhere.[11] The ionic projectiles are produced by heating a specifically designed alkali aluminosilicate salt (HeatWave Labs, Inc.). The ion-beam line provides 1–80 keV mass-analyzed projectiles which interact with the target in an ultrahigh vacuum chamber (base pressure of about 10^{-10} mbar). The target is mounted on a three-dimensional (3D) sample manipulator which allows for variations of both incidence and azimuthal angles. The reflected and recoil particles travel through a 618 mm long time of flight (TOF) spectrometer which can be rotated in the plane of incidence between 0° and 165° and with an acceptance angle of less than 0.5°. At the end of the flight tube, the positive, negative, and neutral particles are separated by a set of deflection plates, the voltage of which is tuned according to the parti-

 ©2007 The American Physical Society

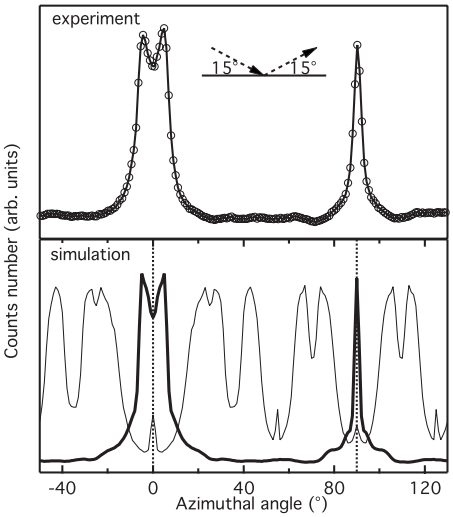

FIG. 1. Comparison between experiment (line with circles) and simulation (thick line) of the number of Ar particles scattered off an Ag(110) surface as a function of the incidence azimuthal angle. Projectiles are 4 keV Ar^+ ions under an incidence angle with respect to the surface $\alpha=15°$. The particles are detected in the specular scattering angle $\theta=30°$. The thin line added in the simulation view corresponds to a different collision geometry: $\alpha=3°$ (grazing angle) and $\theta=6°$.

cle's kinetic energy: the positive and negative ions are deflected on each side of the spectrometer axis. About 70 mm downstream, the particles encounter a two-stage 50 $\times 8$ mm^2 rectangular multichannel plate and a three-part anode assembly. The signal on the small central part of the anode corresponds to the detection of neutrals and those on each side to the detection of charged particles. The three charge types are thus recorded simultaneously in the acquisition system which calculates in real time the corresponding charge fractions.

The Cu and Ag samples (monocrystals with an orientation accuracy better than 1° from the Mateck company) are prepared *in situ* by cycles of grazing-incidence (3°–15°) sputtering with 4 keV Ar^+ ions and annealing at about 800 K (the temperature is then slowly decreased to avoid any freezing of defects). The surface cleanliness is checked by recording TOF spectra of the scattered and emitted particles with a 4 keV Ar^+ pulsed beam under an incidence angle with respect to the surface $\alpha=15°$, verifying the absence of any recoil atom other than Cu or Ag.

To determine accurately the orientation of the target, by using the same 4 keV Ar^+ beam under $\alpha=15°$, we have recorded the number of Ar particles scattered off the surface in the specular direction (exit angle with respect to the surface $\beta=15°$ in the incidence plane) as a function of the azimuthal angle of incidence. As can be seen in the upper panel of Fig. 1 in the case of Ag(110), two characteristic peaks are observed in orthogonal azimuthal directions. Similar results are obtained for the Cu(110) surface. The assignment of these peaks to different target orientations is based on comparisons with simulations realized with the MARLOWE code.[12] This code is based on the binary-collision approximation. The Ziegler-Biersack-Littmark potential[13] was used for the calcu-

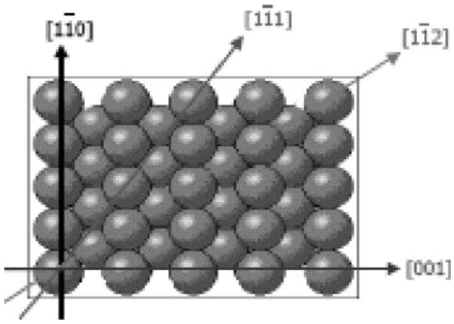

FIG. 2. The low-index crystallographic directions for an fcc (110) surface.

lation shown in Fig. 1 (bottom view). It shows good agreement with the experimental result and allows the [001] and [1$\bar{1}$0] directions to be identified. Better agreement could be obtained by varying the different simulation parameters, in particular, the interaction potential such as the Molière potential with Firsov screening length[14] but this is beyond the scope of this study. It should be noted that, with such an incidence angle of 15°, the number of projectiles scattered in the specular direction is greatest in the [001] and [1$\bar{1}$0] directions because the projectiles are guided along these directions (axial channeling) before exiting the surface, whereas most projectiles are lost inside the crystal for a so-called "random" direction. The situation is reversed for grazing-incidence angles. All projectiles are scattered in the specular direction for a random azimuthal angle, the surface acting as a mirror (planar channeling), whereas the projectiles which impinge along the low-index directions bump from one wall to another of the seams between rows of atoms: as a result, they are dispersed outside the incidence plane, leading to a loss of scattered particles in the specular direction (see thin line in Fig. 1).

III. EXPERIMENTAL RESULTS

To reveal the possible role of the azimuthal angle of incidence on the charge-transfer process, we have chosen the (110) surfaces of Cu and Ag. Note that a (110) surface presents very different interatom distances along the [001] and [1$\bar{1}$0] crystallographic directions (Fig. 2). The atoms are separated by 2.55 Å along the [1$\bar{1}$0] direction but by 3.61 Å along the [001] direction for the Cu (110) surface, or by 2.89 Å and by 4.09 Å, respectively, for the Ag(110) surface. We have focused our study in the vicinity of these directions where evenly spaced rows of atoms lead to a channeling power.

We have measured the charge fractions resulting from the interaction of different projectiles with these two surfaces as a function of the azimuthal angle of incidence. For low incidence angles ($\alpha=3°-5°$) and projectile energies lower than 4 keV, significant variations of the positive charge fraction have been observed for the systems Li^+/Cu and Na^+/Ag in the vicinity of the low-index directions, as shown in the left part of Fig. 3 around the [001] direction. No variation could be measured for the Na^+/Cu system.

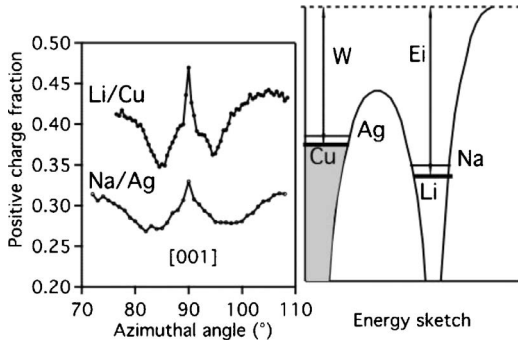

FIG. 3. Left panel: Positive charge fraction as a function of the azimuthal angle of incidence for the scattering of 1.24 keV Li^+ ions on Cu(110) (upper curve) and of 1.24 keV Na^+ ions on Ag(110) (lower curve). The incidence angle is $\alpha=3°$ with respect to the surface and the scattering angle is $\theta=6°$ (specular reflection). The azimuthal angle is measured with respect to the $[1\bar{1}0]$ direction. Right panel: Sketch of energy diagrams for Li and Na atoms in front of Cu and Ag (110) surfaces.

It should be noted that the measurements are very sensitive to the collision geometry. In our experiment, the incidence angle α (position of the target with respect to the beam) and the scattering angle θ (position of the spectrometer with respect to the beam) are fixed to the desired values, then we fine tuned the incidence angle in order to obtain the best symmetric spectra of scattered particles, disregarding their charge, around the low-index directions of the crystal.

The systems under study are very similar from an energetic point of view (right-hand part of Fig. 3), with an ionization energy of the projectile of 5.39 eV for lithium (5.14 eV for sodium) and the Fermi level of the target measured with respect to the vacuum level at 4.5 eV for Cu (4.3 eV for Ag). Neutralization of the projectile by a resonant electronic transfer can take place, provided that the atomic level of the projectile is lower than the Fermi level of the target. However, because of the image-charge interaction of an atom in front of a metal surface,[15] the ionization energy E_i of the projectile is reduced as the distance between the projectile and the surface decreases, and the projectile is reionized very near the surface. A static description of this effect by $E_i(z_i)=E_i(\infty)-\frac{1}{4z_i}$ is a good approximation, with z_i the distance between the projectile and the image plane. The similarity of the atomic and Fermi levels in the systems we have studied leads to a competition between neutralization and reionization, resulting in positive charge fractions in the 30%–70% range.

For 1.24 keV projectile energies, a relative variation of 10%–20% of the positive charge fraction is observed around the [001] direction with respect to a random direction, with three different components: (1) a narrow peak in the axial direction, (2) a dip extending for about 5° on each side, and (3) a monotonic variation when the azimuth differs by more than 10° from the axial direction, approaching the so-called random azimuth and surface- (planar-) channeling conditions. Similar variations have been recorded in the $[1\bar{1}0]$ direction, as shown in Fig. 4 for the Li/Cu system at different projectile energies.

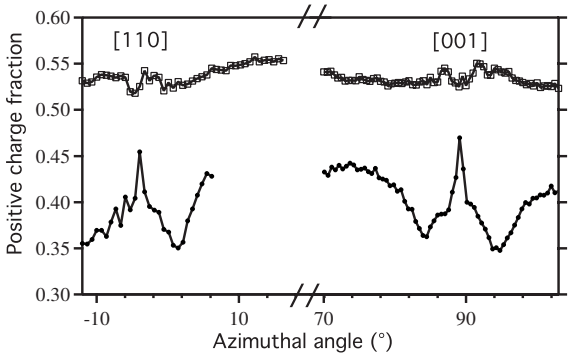

FIG. 4. Energy dependence of the azimuthal variations in the positive charge fraction, for grazing scattering from Cu(110) of 1.24 keV (lower curves) and 4 keV (upper curves) Li ions. The incidence angle is $\alpha=3°$ with respect to the surface and the scattering angle is $\theta=6°$ (specular reflection). Note the split of the horizontal azimuthal axis.

The significant variation of the charge fraction at 1.24 keV disappears for 4 keV ions. The azimuthal variations in the charge fraction depend sensitively on the incidence angle, as seen in Fig. 5 for three different angles in the case of 1.24 keV Li^+ ions from Cu(110) and in Fig. 6 in the case of 2 keV Na^+ ions from Ag(110): the variations vanish when the angle is increased. This implies that these variations are somehow related to the parallel and/or perpendicular velocities of the projectiles.

IV. DISCUSSION

Cu and Ag are known as good candidates to illustrate the free-electron (or jellium) model to describe the electronic structure of metals. An extensive literature[3,6] has been devoted to the resonant transfer process responsible for neutralization of alkali ions in front of these surfaces. Within the freezing-distance model,[6] the positions of the electron atomic level and of the Fermi level have to be compared only in a small range of projectile-surface distances. This model is based on the comparison of two time scales: the first is in-

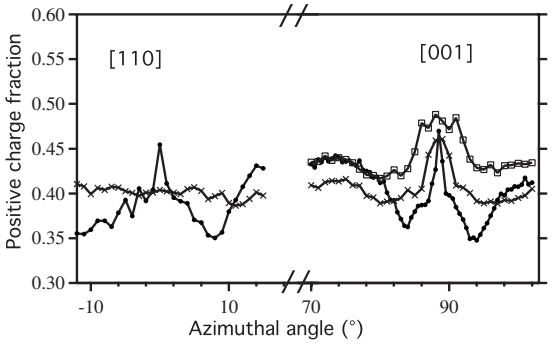

FIG. 5. Positive charge fraction as a function of the azimuthal angle for scattering of 1.24 keV Li^+ from Cu(110). The results correspond to three different angles of incidence: $\alpha=3°$ (full circles), $\alpha=4°$ (crosses), and $\alpha=5°$ (empty squares) and an exit angle in the specular direction.

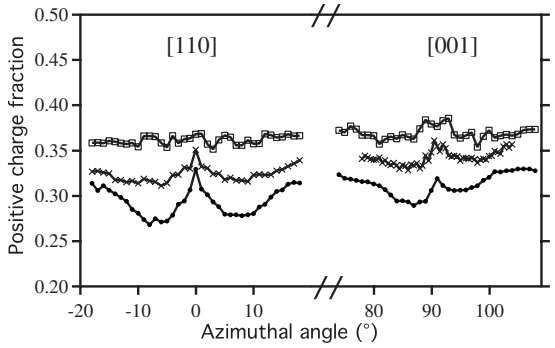

FIG. 6. Positive charge fraction as a function of the azimuthal angle for scattering of 2 keV Na^+ from Ag(110). The results correspond to three different angles of incidence: $\alpha=3°$ (full circles), $\alpha=4°$ (crosses), and $\alpha=5°$ (empty squares) and an exit angle in the specular direction.

versely proportional to the coupling between the surface and the projectile, and the second is the time scale for the atom scattering from the surface. Far from the surface, the coupling between the atom and the surface is weak: no charge transfer occurs. On the other hand, charge-transfer rates are large very near to the surface: any memory of the initial charge state is lost. As a consequence, the exit charge state of the projectile is determined on its exit in a small range of projectile-surface distances, around the so-called "freezing distance" where the two time scales are of the same order. It can be shown that the probability P_n of electron capture by the projectile on its exit corresponds to the equilibrium occupation of the atomic level at this distance, the positive charge fraction being thus $(1-P_n)$.

The width $\Delta(z)$ of the atomic level in front of a jellium is often approximated by an exponential variation with distance:

$$\Delta(z) = \Delta_0 \exp\left(\frac{-z}{z_0}\right),$$

where z is the atom-jellium edge distance and Δ_0, z_0 two parameters characteristic of the atom-surface system. The jellium edge is known to be located in front of the surface at about half the interlayer distance from the first atomic layer, that is, 1.1 a.u. for Cu(110).

The freezing distance, measured with respect to the image plane, is given by

$$z_f = z_0 \ln\left(\frac{\Delta_0 z_0}{v_z}\right),$$

where v_z is the perpendicular velocity of the projectile. The image plane, according to different studies, is located between 0.1 and 1 a.u. from the jellium edge (1.2–2.1 a.u. from the first atomic layer).

In a previous paper,[16] we have performed a detailed analysis of the neutralization probability according to the perpendicular and parallel velocities of the projectiles within this model for a random azimuthal angle. The image-charge parameters $\Delta_0=4.46$ a.u. and $z_0=1.16$ a.u. of Onufriev and Marston[17] for the Li/Cu system allowed us to account for the charge-fraction variations over a wide range of energies and/or incidence angles and particularly for the results reported above: as the angle of incidence or the energy increases, the perpendicular energy increases, and thus the charge fraction increases because of the diminution of the freezing distance. This is clearly visible in Figs. 4 and 6. Calculations of neutralization probabilities show that the Δ_0 parameter is less sensitive than z_0. The above value of 1.16 a.u. (Ref. 17) appears as a lower limit as compared to our experimental data. A value of 1.5 a.u. appears to be more consistent with the observed increase of about 10% of the positive charge fraction when comparing 1.24–4 keV projectiles whose incidence angle is 3°. The first value gives neutralization probabilities of 45% and 49% (with a freezing distance around 8 a.u.), whereas the second one gives 48% and 55% (freezing distance around 10 a.u.), in better agreement with the observed increase.

However, the free-electron and freezing-distance models mentioned above do not explain the observed azimuthal variations. It is well known that the substantial variations observed in the azimuthal spectra of the number of scattered particles in the specular direction under grazing incidence are due to the corrugation of the surface, which thus does not match a perfect jellium model. The projectiles, according to their impact point on the target, do not follow the same trajectories and can be scattered outside the specular angle. In order to obtain a better comprehension of our experimental results, we have performed computer simulations of projectile trajectories using the binary-collision approximation MARLOWE code. It has been shown to give similar results to molecular dynamics codes[4] even in grazing geometries, and is significantly faster: running the code for a whole set of azimuthal angles allows us to construct the azimuthal spectra point per point, for a given collision geometry and interaction potential. In the code, as soon as a "collision" is identified by a very small energy change of the projectile, its position is recorded in order to yield the projectile trajectory: in grazing scattering conditions, about ten crystal atoms are involved in the collision sequence with distances of closest approach that are less than half the lattice constant (around 3 a.u.).

Typical trajectories under axial channeling conditions are plotted in Fig. 7. Only the trajectories corresponding to scattered particles in the specular direction are represented (acceptance angle of 0.4°). They can be split in three types: on top, in row, and zigzag ones, similar to those obtained for other systems.[4,18] On-top trajectories do not penetrate the crystal, just as the trajectories obtained for planar channeling. As opposed, in-row and zigzag trajectories can dip under the first atomic layer, in the seam between two atomic rows; in rows are long guided straight trajectories whereas zigzag trajectories arise from successive reflections on the walls of the seam. In rows penetrate deeper than zigzags and vanish quite fast when rotating the crystal out of the axial channel, but zigzags survive up to 5°–8° apart from the axial direction.

Such trajectory simulations have allowed us, in the case of grazing scattering of F^+ ions on a NaCl surface, to link the azimuthal variations of the negative charge fraction to the number of Cl^- ions visited and in the case of grazing scat-

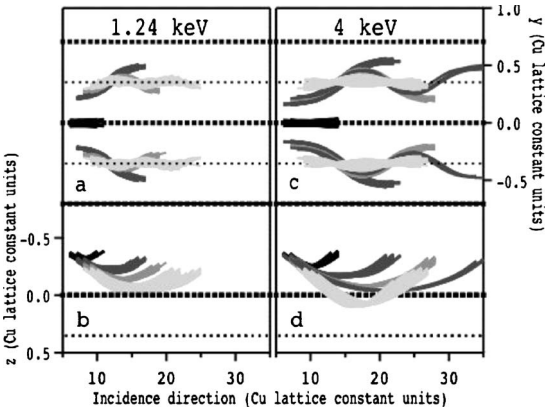

FIG. 7. Calculated trajectories of 1.24 and 4 keV Li atoms scattered under grazing incidence from a Cu(110) surface. The incidence angle is $\alpha=3°$ with respect to the surface, the azimuthal angle is along the [001] direction, and the scattering angle is $\theta=6°$ (specular reflection). (a) and (c) are top views of the crystal surface; (b) and (d) are side views along the incidence direction. The gray scale allows one to distinguish between the different types of trajectories. Atoms of the first and second layers are represented by dots. The scale in the direction of incidence is shrunk; the lengths are expressed in unit of the lattice constant (3.62 Å for Cu). These simulations have been done without thermal effects in order to distinguish more clearly between the different trajectories. They have been performed with a modified Molière potential (adjustment of the screening length by a factor of 0.85).

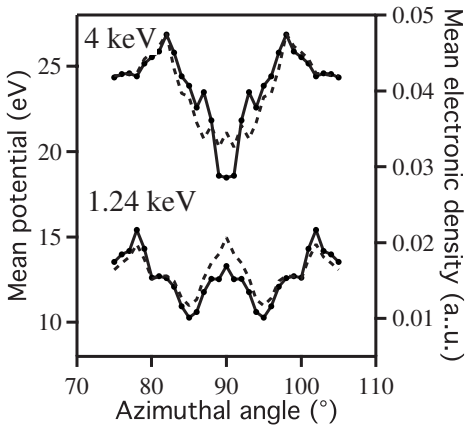

FIG. 8. Mean interaction potential (line with markers and left axis) and mean electronic density (dotted line and right axis) encountered by 1.24 and 4 keV Li projectiles impinging on Cu(110) with an $\alpha=3°$ grazing angle at different azimuthal angles.

tering of Ne^+ ions to link the positive charge fraction to the number of Na^+ ions visited,[4] these results being consistent with the strongly localized electronic density around the ionic cores in insulators. We did not succeed in establishing such a link for the systems studied here: the charge-transfer process appears to be more sensitive to the electronic corrugation as a whole rather than to the ion core positions of the Ag(110) and Cu(110) surfaces.

To obtain a correlation between the projectile trajectories and the electronic corrugation, as in the work of Robin *et al.*[18] on the correlation between electronic stopping and density corrugation, we have made a further analysis of the trajectories. The geometry of the (110) surface induces different distributions of the electronic density along the different crystal axes and different interaction potentials between the projectile and the crystal atoms. Therefore, the collision time, which can be associated with a mean "effective" perpendicular energy, should be different for projectiles according to the way they follow the surface, straight along a seam, bumping from one wall to another or randomly. The freezing-distance model, based on the free-electron description of the metal with a flat hard repulsive wall, assumes a constant absolute value of the perpendicular velocity (constant collision time) and does not include such trajectory effects.

Our simulations reveal that most of the trajectories penetrate into regions where the interaction potential is higher than their initial perpendicular energy far from the surface. The trajectories of Fig. 7 show that along the [001] direction, in-row trajectories (light gray) remain above the first atomic layer for an incident perpendicular energy lower than 10 eV (left-hand side $E_z=3.4$ eV), whereas they dip under the first layer for higher energies (right-hand side $E_z=10.9$ eV). The azimuthal variations of the charge fraction occur around the low-index directions, when on-top, zigzag, and in-row trajectories are possible and disappear for perpendicular energies greater than about 10 eV, when the trajectories dip under the first atomic layers. Similar trajectories as those on the right-hand side, although shorter, are obtained for 1.24 keV with $\alpha=5°$ ($E_z=9.4$ eV). The proportions of in rows are about 30% for a perpendicular energy less than 10 eV, whereas they are more than 60% for a perpendicular energy around 10 eV. For random directions, trajectories remain at a distance of 0.2–0.3 times the lattice constant but they can encounter high potential values by cutting through the bumps. For all the collision points which define the projectile trajectory, we have calculated the corresponding interaction potential used in the MARLOWE code. The mean values of these potentials, calculated for a meaningful number of trajectories, are plotted in Fig. 8 for 1.24 keV and for 4 keV Li projectiles interacting with Cu(110) ($\alpha=3°$) and at different azimuthal angles around the [001] direction. They are clearly above the E_z values.

The comparison of the curves of Fig. 8 with the experimental azimuthal variations shown in Fig. 4 yields a reasonable agreement: a dip on each side of the [001] direction at 1.24 keV and a dip in this direction at 4 keV. These variations are closely related to the respective proportions of the different types of trajectories, according to the energy and the angle of incidence of the projectile. The in-row trajectories disappear when turning out of the [001] direction, whereas the zigzag ones become important some 5° away from this direction, before vanishing, leaving only planar channeling trajectories.

Although it is difficult to relate the surface electronic corrugation to the interaction potential, we have performed electronic density calculations on a 3D grid for Cu(110) using density functional theory (DFT), at least for the first layers.[19] We have compared, in the vicinity of the surface, several contours of constant density with the isovalue contours of the

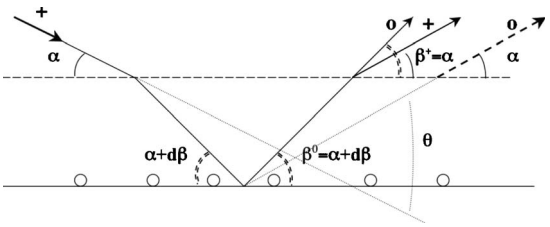

FIG. 9. Illustration of the image-charge effect on a projectile trajectory: case of an impinging positive ion which can be neutralized during scattering. In the case of a pure specular reflection, the exit angle of the projectile will be $\beta^0=\alpha+d\beta$ if scattered as a neutral and $\beta^+=\alpha$ if scattered as an ion.

sums of the different interaction pair potentials used in MARLOWE. Those obtained with a modified Molière potential are very, although not strictly, similar to those obtained by DFT, which shows that the above simulations are reliable. From the above 3D grid, the electronic density value for each point defining a trajectory is known, and we can thus estimate the mean electronic density (in a.u.) visited by the projectile during its flight over the surface (dotted line in Fig. 8). To ascertain and quantify such a correlation between the variations in azimuthal charge fraction and electronic density, trajectories must be calculated by molecular dynamics (MD) with potentials more appropriate than the pair potentials we have used. Recently, Karolewski[20] has shown that the Molière potentials are too repulsive below 1–2 keV and that corrections deduced from DFT calculations improve the accuracy of the MD predictions.

The above analysis shows that in channeling conditions, depending on the azimuthal angle, the electronic density seen by the projectile depends strongly on the trajectory and this could result in charge-fraction variation. However, this effect occurs near the surface (below 3 a.u.), in contradiction with the well-established freezing-distance model, in which the charge state is determined far from the surface (8–10 a.u.) and which gives a good prediction of the mean value of the charge fraction. The question is how this short-distance effect can be observed in the outgoing trajectories?

During grazing scattering on a flat surface, an image-charge attractive potential affects the trajectories of ingoing and outgoing ions, whereas the neutrals are insensitive to this potential. It has been shown[3,21,22] that when charge exchange occurs under very small grazing angles ($\alpha<1°$), neutrals and positive ions are observed at slightly different angles (Fig. 9), the difference between their exit angles being approximated by the expression

$$d\beta = \beta^0 - \beta^+ = \beta^0\left(1 - \sqrt{1 - \frac{E_i}{E_z}}\right),$$

where E_z is the perpendicular energy of the incident particles and E_i the image-charge potential at the freezing distance.

Therefore, with a fixed detection angle (scattering angle θ), the detected neutral and ionized particles have followed different trajectories and have experienced different electronic densities. In the vicinity of low-index directions, the scattered intensity in a given solid angle varies quickly with

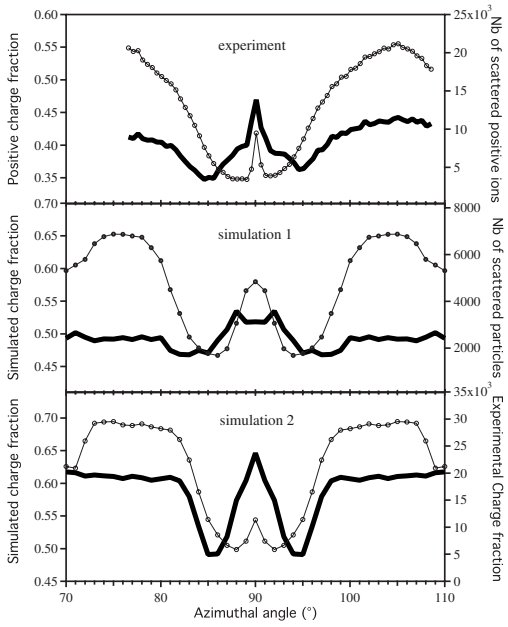

FIG. 10. Comparison of azimuthal variations of the charge fraction (bold line) and of the number of scattered positive ions (lines with markers) between experiment (top view) and two simulations (lower views). Experiment: 1.24 keV Li ions on Cu ($\alpha=3°$ and $\beta=3°$). Simulation 1: $\alpha=3°$ and $d\beta=0.3°$; simulation 2: $\alpha=1.3°$ and $d\beta=0.5°$ (see text).

azimuth and depends on the incidence and exit angles, so the azimuthal variations of the number of detected ions n_+ and of detected neutrals n_0 will be different. As a consequence, even if the total numbers of scattered ions and neutrals are equal, the apparent charge fraction, measured as $n_+/(n_++n_0)$, will vary with the azimuthal angle. This effect disappears with increasing energy and/or incidence angle, since the $d\beta$ shift decreases rapidly, in agreement with our observations (data in Figs. 4–6).

To estimate such azimuthal variations, we have performed trajectory simulations with different incidence and exit angles, for a series of azimuthal angles. Since the MARLOWE code deals only with neutral projectiles, the deflection of ions by the image-charge effect, cannot be introduced directly. To simulate this effect, we have performed two sets of simulations: one for the "neutrals" and one for the "ions." For an ionic beam striking the surface with a given incidence angle α, the effective angle of incidence on the surface is $\alpha+d\beta$, because of the image-charge effect. If the scattered particles are neutrals, they will be "specularly" reflected by the angle $\beta=\alpha+d\beta$ (resulting in a scattering angle $\theta=2\alpha+d\beta$), whereas the ions will be specularly reflected with $\beta=\alpha$ ($\theta=2\alpha$), due to the inverse image-charge effect. Because all of the collisions in MARLOWE occur below the freezing distance, the angle of incidence in the code is taken equal to the effective incidence angle. One runs the code at different azimuthal angles to obtain the azimuthal spectrum of reflected species for each set (typically 100 000 projectiles for each angle and each set).

Under our experimental conditions, with initial energies of 1.24–4 keV and incidence angles with respect to the sur-

face of 3°–5°, the perpendicular velocity ranges from 0.004 to 0.013 a.u., resulting in a freezing distance z_f of about 8–10 a.u. and an angular difference between scattered ions and neutrals $d\beta$ less than 0.35°, this upper limit corresponding to 1.24 keV, $\alpha=3°$, and $z_f=8$ a.u. In Fig. 10, two simulations are compared with experimental data points recorded for 1.24 keV Li+ scattered on Cu(110) with $\alpha=3°$.

Simulation 1 was performed with the experimental collision geometry and $d\beta=0.3°$ (calculated with the above formula with a freezing distance between 8 and 10 a.u.), that is, a scattering angle $\theta=6°$, effective $\alpha=3.3°$, $\beta=3.3°$ and $\alpha=3.3°$, $\beta=3°$ to simulate ions and neutrals, respectively. The simulations were performed with a modified Molière interaction potential following common practice in the ion-scattering community[23] (screening length adjusted by a factor of 0.75), by including thermal effects ($T=300$ K and Debye temperatures of 300 K along the close packed row [110] and 200 K along the [001] and perpendicular directions) and taking into account the experimental detection resolution of 0.4°. None of the potentials available in MARLOWE (as sum of diatomic interaction potentials) yields an exact fit of the variation of the number of scattered projectiles: the wells around the low-index directions are somehow too wide (see simulation 1). Their widths vary more quickly for lower incidence angles. Simulation 2 of Fig. 10, performed with a lower scattering angle $\theta=2.6°$, taking effective $\alpha=1.8°$, $\beta=1.8°$ and $\alpha=1.8°$, $\beta=1.3°$ to simulate ions and neutrals, respectively, gives well widths for the scattered ions identical to the experimental ones. In both simulations, the apparent charge fraction, given by the ratio $n_+/(n_++n_0)$, shows azimuthal variations of the same order as the experimental data, although its value by itself, based on an equal number of neutral and ionic projectiles thrown on the surface, has no actual meaning.

Although the $d\beta$ shift must be increased from the estimated value of 0.3–0.5° for a qualitative agreement in the case above, and although similar behavior is observed for higher α angles for which $d\beta$ is even lower, the simulations show that azimuthal variations in the charge fraction arise from different azimuthal variations of the number of positive and neutral particles, because the ions and the neutrals detected at a given angle arise from different collision geometries. This can be observed for systems in which there is a balance between neutralization and ionization (charge fraction around 50%); otherwise, the azimuthal variation of the minor part will be hidden under the major one. This is in agreement with the fact that we do not observe any azimuthal variations for the Na/Cu system (positive charge fraction above 70% in the 1.24–4 keV range).

V. CONCLUSION

We have experimentally observed azimuthal variations of positive charge fractions in the grazing scattering of 1.24–4 keV Li^+ and Na^+ projectiles on Ag(110) and Cu(110) surfaces. This is rather surprising for metallic surfaces as opposed to insulator surfaces: the latter, due to a strong electronic corrugation, produce different charge-transfer probabilities according to whether the projectile trajectory goes near an ionic core or not. The recorded variations on the metallic surfaces are very sensitive to the initial energy of the projectiles and require grazing-incidence conditions.

From a detailed analysis of trajectory calculations, two reasons for these experimentally observed variations are given. As the projectiles follow different classes of trajectories according to their azimuthal angles of incidence and impact points on the surface, the electronic densities encountered are different. We have shown, with a simple superposition of trajectories with electron density contours calculated by DFT, that the mean electronic density visited and the observed charge fraction vary in a similar way with the azimuthal angle, thus establishing a link between the electronic density and the neutralization probability. This effect occurs near the surface (below 3 a.u.).

This effect reflects itself in the outgoing trajectories, in agreement with the long-range model in which the charge state is determined far from the surface (8–10 a.u.), through the image-charge effect: the ions and the neutrals detected in a given solid angle correspond to projectiles scattered under different "effective" exit angles (under surface axial channeling, the incident beam is dispersed over a whole range of exit angles). As a consequence, their numbers vary slightly differently according to the azimuthal angle of incidence, leading to a variation in the measured charge fraction. With computer simulations based on a binary-collision approximation and modified Molière interaction potentials, we have succeeded in reproducing the observed experimental variations. Molecular dynamics calculations with potentials derived from accurate density calculations should be performed in order to verify this result.

By extension of our study, azimuthal charge-fraction variations are expected for systems in which the ionization energy of the projectile exceeds the work function of the surface by about 0.8 eV, resulting in a positive charge fraction in the 30%–70% range. For these systems, the comparison of experimental azimuthal charge-fraction variations with MD trajectory calculations appears to be a suitable method to investigate the electronic corrugation of the surface.

ACKNOWLEDGMENTS

We thank N. Lorente for discussions and help to obtain the electronic density of Cu(110) and C. Marsden for rereading the manuscript.

*Corresponding author; martine.richard-viard@irsamc.ups-tlse.fr

[1] J. Los and J. J. C. Geerlings, Phys. Rep. **190**, 133 (1990).
[2] B. H. Cooper and E. R. Behringer, in *Low Energy Ion-Surface Interactions*, edited by J. Rabalais (Wiley, New York, 1994).
[3] H. Winter, Phys. Rep. **367**, 387 (2002).
[4] M. Richard-Viard, S. Abidi, C. Bénazeth, P. Benoit-Cattin, and P. Cafarelli, Nucl. Instrum. Methods Phys. Res. B **184**, 490 (2001).
[5] H. Winter, Prog. Surf. Sci. **63**, 177 (2000).
[6] E. G. Overbosch, B. Rasser, A. D. Tenner, and J. Los, Surf. Sci. **92**, 310 (1980).
[7] G. A. Kimmel and B. H. Cooper, Phys. Rev. B **48**, 12164 (1993).
[8] C. A. Keller, C. A. DiRubio, G. A. Kimmel, and B. H. Cooper, Phys. Rev. Lett. **75**, 1654 (1995).
[9] V. A. Morozov and F. W. Meyer, Phys. Rev. Lett. **86**, 736 (2001).
[10] R. Monreal, E. C. Goldberg, F. Flores, A. Närman, H. Derks, and W. Heiland, Surf. Sci. **211**, 271 (1989).
[11] C. Bénazeth, P. Benoit-Cattin, P. Cafarelli, P. Reynes, J. Ziesel, and N. Bénazeth, Nucl. Instrum. Methods Phys. Res. B **94**, 581 (1994).
[12] M. T. Robinson, Phys. Rev. B **40**, 10717 (1989).
[13] W. Eckstein, *Computer Simulations of Ion-Solid Interactions* (Springer, New York, 1991).
[14] G. Molière, Z. Naturforsch. A **2A**, 133 (1947).
[15] H. Winter, J. Phys.: Condens. Matter **8**, 10149 (1992).
[16] N. Nieuwjaer, C. Bénazeth, P. Benoit-Cattin, P. Cafarelli, and M. Richard-Viard, Nucl. Instrum. Methods Phys. Res. B **230**, 317 (2005).
[17] A. V. Onufriev and J. B. Marston, Phys. Rev. B **53**, 13340 (1996).
[18] A. Robin, A. V. Postnikov, and W. Heiland, Surf. Interface Anal. **37**, 154 (2005).
[19] N. Lorente (private communication).
[20] M. Karolewski, Nucl. Instrum. Methods Phys. Res. B **243**, 43 (2006).
[21] H. Winter, Phys. Rev. A **46**, R13 (1992).
[22] H. Winter and J. Leuker, Nucl. Instrum. Methods Phys. Res. B **72**, 1 (1992).
[23] Th. Fauster, D. Hartwig, and H. Durr, Appl. Phys. A: Solids Surf. **45**, 63 (1988).